Published in final edited form as:

N Engl J Med. 2015 March 19; 372(12): 1126–1137. doi:10.1056/NEJMoa1400116.

Brain Swelling and Death in Children with Cerebral Malaria

Karl B. Seydel, M.D., Ph.D, **Samuel D. Kampondeni, M.B., Ch.B**, **Clarissa Valim, M.D., D.Sc**, **Michael J. Potchen, M.D**, **Danny A. Milner, M.D**, **Francis W. Muwalo, A.D.I.T**, **Gretchen L. Birbeck, M.D**, **William G. Bradley, M.D., Ph.D**, **Lindsay L. Fox, M.D**, **Simon J. Glover, F.R.C. Ophth**, **Colleen A. Hammond, A.S**, **Robert S. Heyderman, F.R.C.P., Ph.D**, **Cowles A. Chilingulo, B.Sc**, **Malcolm E. Molyneux, F.Med.Sci**, and **Terrie E. Taylor, D.O.**

Department of Osteopathic Medical Specialties, College of Osteopathic Medicine (K.B.S., L.L.F., T.E.T.), Department of Radiology (M.J.P., C.A.H.), and Department of Neurology and Ophthalmology, International Neurologic and Psychiatric Epidemiology Program (G.L.B.), Michigan State University, East Lansing; the Blantyre Malaria Project (K.B.S., S.D.K., D.A.M., F.W.M., L.L.F., T.E.T.) and Malawi– Liverpool–Wellcome Trust Clinical Research Programme (R.S.H., M.E.M.), Queen Elizabeth Central Hospital (S.D.K., C.A.C.) and the Department of Anatomy (S.J.G.), University of Malawi College of Medicine — both in Blantyre, Malawi; the Department of Immunology and Infectious Diseases, Harvard School of Public Health (C.V., D.A.M.), and the Department of Pathology, Brigham and Women's Hospital (D.A.M.) — both in Boston; the Department of Radiology, University of California San Diego, San Diego (W.G.B.); and the Liverpool School of Tropical Medicine, Liverpool, United Kingdom (M.E.M.).

Abstract

BACKGROUND—Case fatality rates among African children with cerebral malaria remain in the range of 15 to 25%. The key pathogenetic processes and causes of death are unknown, but a combination of clinical observations and pathological findings suggests that increased brain volume leading to raised intracranial pressure may play a role. Magnetic resonance imaging (MRI) became available in Malawi in 2009, and we used it to investigate the role of brain swelling in the pathogenesis of fatal cerebral malaria in African children.

METHODS—We enrolled children who met a stringent definition of cerebral malaria (one that included the presence of retinopathy), characterized them in detail clinically, and obtained MRI scans on admission and daily thereafter while coma persisted.

RESULTS—Of 348 children admitted with cerebral malaria (as defined by the World Health Organization), 168 met the inclusion criteria, underwent all investigations, and were included in the analysis. A total of 25 children (15%) died, 21 of whom (84%) had evidence of severe brain swelling on MRI at admission. In contrast, evidence of severe brain swelling was seen on MRI in 39 of 143 survivors (27%). Serial MRI scans showed evidence of decreasing brain volume in the survivors who had had brain swelling initially.

Address reprint requests to Dr. Taylor at Michigan State University, W. Fee Hall, 909 Fee Rd., Rm. B305-B, East Lansing, MI 48824, or at ttmalawi@msu.edu.

CONCLUSIONS—Increased brain volume was seen in children who died from cerebral malaria but was uncommon in those who did not die from the disease, a finding that suggests that raised intracranial pressure may contribute to a fatal outcome. The natural history indicates that increased intracranial pressure is transient in survivors. (Funded by the National Institutes of Health and Wellcome Trust U.K.)

Despite recent advances in treatment, prevention, and control, malaria remains a major scourge.[1] Quinine, the mainstay of treatment for cerebral malaria for 300 years, has been supplanted by artesunate,[2,3] but despite more rapid parasite clearance with artesunate, the case fatality rate among African children with cerebral malaria treated with arte-sunate remains high at 18%.[3] Improvements in community-based care will help to prevent cerebral malaria, but additional advances in the treatment of hospitalized patients will probably require adjunctive therapies targeting key pathogenetic mechanisms.

The pathogenesis of cerebral malaria is incompletely understood, and although there is considerable evidence to suggest that the processes differ in adults and children,[4,5] most hypotheses encompass a feature of the parasite life cycle that is unique to *Plasmodium falciparum*: the sequestration of parasitized erythrocytes in the microvasculature of various organs, including the brain.[6] The ramifications of sequestration with potential pathogenetic significance include vascular congestion,[7] impaired perfusion,[8] endothelial-cell activation,[9,10] which may lead to breakdown of the blood–brain barrier[11] and cerebral edema,[12] and a systemic inflammatory response[13,14] resulting in a prothrombotic state.[15–19]

Until recently, the identification of the critical pathogenetic mechanisms has been complicated by an imprecise clinical case definition. Findings from a large autopsy-based study of clinicopathological correlates in cerebral malaria showed that up to 25% of children who met the standard clinical case definition of cerebral malaria[20] did not have histologic evidence of sequestration at autopsy.[6] Nonmalarial causes of death were identified in each case. A constellation of ocular funduscopic findings, known collectively as malarial retinopathy, reliably distinguishes malarial coma from nonmalarial coma during life, and the inclusion of eye findings in the clinical case definition significantly improves its specificity without compromising sensitivity.[21,22]

The same autopsy-based study showed that increased brain weight–for–age was nearly ubiquitous among patients who died with clinically defined cerebral malaria, with or without sequestration, but there were no consistent gross pathological findings implicating raised intracranial pressure as a cause of death.[6] Earlier studies involving African children with cerebral malaria, in which intracranial pressure was monitored directly, showed raised intracranial pressure,[12,23] and a study of computed tomographic (CT) imaging in children with acute cerebral malaria showed significantly increased brain volume in 6 of 14 children[24]; however, in order to determine the association between increased brain volume and death definitively, larger numbers of well-characterized patients and comparisons with survivors were needed. For these reasons, we added magnetic resonance imaging (MRI) studies to the clinical characterization of children with retinopathy-positive cerebral malaria in Blantyre, Malawi.

METHODS

STUDY DESIGN

This observational study was performed at the Queen Elizabeth Central Hospital in Blantyre, Malawi, from January 2009 through June 2011. All children older than 5 months of age who met the clinical case definition of cerebral malaria (Blantyre coma score ≤2, on a scale from 0 to 5, with lower scores indicating decreased levels of consciousness; peripheral parasitemia with *P. falciparum* of any density; and no other discernible cause of coma) were identified and cared for in a high-dependency ward. Patients were treated with intravenous quinine (according to national guidelines at the time) and adjunctive measures as needed. Mechanical ventilation was not available. A trained ophthalmologist performed ocular funduscopy within 6 hours after admission.

Venous blood was drawn on admission to obtain a complete blood count (Coulter Counter, Beckman Coulter) and blood culture (BACTEC 9120, Becton Dickinson). We analyzed finger-prick samples to determine the parasite species and density, packed-cell volume, and blood glucose and lactate concentrations. Status with respect to human immunodeficiency virus (HIV) infection was determined with the use of two rapid tests: Uni-Gold Recombigen HIV-1/2 (Trinity Biotech) and Determine HIV-1/2 (Inverness Medical). A lumbar puncture was performed unless, in the judgment of the admitting clinician, it was contraindicated. The opening pressure was measured with the use of a flexible manometer,[25] and the cerebrospinal fluid (CSF) was analyzed (cell count, Gram's staining, and culture) with the use of standard methods.[26] Further details of the study are provided in the protocol (including the statistical analysis plan), available with the full text of this article at NEJM.org.

STUDY OVERSIGHT

This study was approved by the research ethics committee at the University of Malawi College of Medicine and by the institutional review board at Michigan State University. On admission of the patient to the hospital, written informed consent was obtained from an accompanying parent or guardian.

MRI SCANS

Scans were performed with the use of the 0.35-T Signa Ovation Excite MRI scanner (General Electric) (Table S2 in the Supplementary Appendix, available at NEJM.org). Two radiologists, who were unaware of each other's readings and of the patient's retinopathy status and clinical outcome, interpreted each MRI study. Adjudication was performed by the two radiologists as required on the basis of prespecified criteria.[27] Overall brain volume was scored on the basis of the appearance of the cerebral hemispheres on a scale from 1 to 8, with a score of 1 indicating marked atrophy, 2 mild atrophy, 3 normal volume, 4 slightly increased volume, 5 mildly increased volume, 6 obvious but moderate levels of increased brain volume, 7 substantially increased volume with diffuse sulcal and cisternal effacement but no evidence of herniation, and 8 sulcal and cisternal effacement with evidence of herniation. Volume scores of 7 and 8 were prespecified as severely increased brain volume because the radiologists considered these scores to indicate a life-threatening condition.

A previously described lobar distribution of MRI abnormalities[28] (anterior or homogeneous vs. predominantly posterior cerebral) was noted. The amount of CSF surrounding the brain stem is inversely related to brain volume, and two objective measures on a sagittal MRI scan were made (Fig. 1): the anterior–posterior dimension of the postpontine space, which quantifies CSF in the fourth ventricle, and the anterior–posterior dimension of the prepontine space, which represents CSF in the subarachnoid space.

ELECTROENCEPHALOGRAPHY

Electroencephalograms (EEGs) were recorded on the day of admission by means of a Ceegraph digital machine (BioLogic) with the use of a modified 10–20 system that met the guidelines of the American Clinical Neurophysiology Society.[29] EEGs were systematically reviewed by a neurologist with fellowship training in EEG who was unaware of the patients' retinopathy status and outcome. The assessed EEG characteristics included the dominant background rhythm, the average background amplitude excluding vertex sharp waves (sharp waves from the vertex that occur in association with normal sleep) and epileptiform activity (<60 μV vs. ≥60 μV), the presence or absence of normal sleep architecture (which included assessments of vertex sharp waves, sleep spindles, and K complexes), and reactivity (present vs. absent).

STATISTICAL ANALYSIS

The clinical characteristics and MRI and EEG features of the children with cerebral malaria who died were compared with those of the children who survived, with the use of Pearson's chisquare tests or Fisher's exact tests for categorical variables and Student's t-tests or Wilcoxon tests for continuous markers. Reliability analyses (kappa statistics and intraclass correlation coefficients) were performed to compare the readings by the two radiologists. The strength of association was measured by means of odds ratios estimated in crude and adjusted logistic-regression models. For logistic-regression models, the linear association of continuous predictors with the logit of death was first evaluated by means of generalized additive models. The selection of relevant markers was based on P values in a Wald test of less than 0.05. With the use of best-subset regression, relevant MRI markers were selected, and then various EEG, clinical, and laboratory variables were evaluated for their predictive capacity. None of the clinical or laboratory variables emerged as independent predictors. For the final model, we reported the P value of the likelihood-ratio test in which models that included each marker were compared with models lacking that specific marker. In addition, we tested all two-way interactions in the final logistic-regression models.

We tried to identify risk factors for important MRI features among the demographic, clinical, laboratory, and EEG variables, using logistic regression in the analysis of categorical variables and linear regression in the analysis of continuous outcomes. Changes over time in the measurements of CSF in the prepontine cistern in the patients who underwent both a baseline MRI and an additional MRI were studied by means of a linear mixed model. In these models, a random intercept and random slope for change in prepontine CSF according to a subsequent MRI scan were included to account for within-patient correlation, and we used an interaction test to determine differences in the slope of trajectories between the patients who died and those who survived.

Statistical analyses were performed with the use of SAS software, version 9.2 (SAS Institute) and R software.[30] P values are two-sided, and P values of 0.05 or less were considered to indicate statistical significance. No adjustment for multiple testing was performed.

RESULTS

STUDY POPULATION

A total of 348 children met the World Health Organization (WHO) criteria[20] for cerebral malaria during the 3-year study period. A total of 85 children did not have retinopathy, and 1 did not undergo funduscopic examination; these children were excluded from the analysis. Of the 262 children who met the strict definition of cerebral malaria (WHO criteria plus retinopathy), imaging was not possible in 46 patients who regained consciousness quickly, 15 who died before imaging was undertaken, and 33 who could not undergo scanning for logistic reasons. The 15 children with retinopathy-positive cerebral malaria who died before undergoing MRI were more likely to have acidosis than were the 168 children who underwent MRI examination, and also had shorter coma-duration times, but otherwise the groups were similar (Table S4 in the Supplementary Appendix). Findings from the 168 children with complete information, including 143 children who survived (85%) and 25 who died (15%), are described here.

CLINICAL AND Imaging FEATURES ASSOCIATED WITH A FATAL OUTCOME

With respect to laboratory test results, only the plasma lactate concentration and white-cell count distinguished children who survived from those who died (Table 1). Among MRI features, severely increased brain volume, decreased prepontine and postpontine CSF levels, predominantly posterior cerebral involvement, supratentorial graymatter lesions, thalamic involvement, and the presence of patchy (vs. confluent) lobar areas of involvement significantly distinguished children who survived from those who died (Fig. 1 and Table 2). The overall agreement between the two radiologists' readings varied from 71 to 96%; the moderate kappa values are attributed to the skewed or unbalanced marginal distributions (Table S3 and Fig. S1 in the Supplementary Appendix).

Among patients with increased brain volume, all those who died had a decreased prepontine CSF level, a predominantly posterior pattern, or both. Among the 25 patients who died in this study, 21 (84%) had brain swelling on the initial MRI (Fig. 2).

The EEG variables associated with a fatal outcome were the absence of normal sleep architecture and reactivity and a median dominant rhythm frequency that was slower than that observed in the patients who survived (Table 2). In an analysis that accounted for MRI, EEG, and clinical factors simultaneously, the final model included three MRI variables (decreased prepontine CSF level, severely increased brain volume, and posterior predominance) and one EEG feature (slower dominant rhythm frequency in the children who died, as compared with those who survived) (Table 2); the associated area under the receiver-operating-characteristic (ROC) curve was 0.90.

PREDICTORS OF MRI ABNORMALITIES ASSOCIATED WITH FATAL OUTCOME

Among all the demographic and clinical factors at the time of admission, increased brain volume was significantly associated with the concentration of lactate (odds ratio, 1.1 per mmol of lactate; P = 0.01), jaundice (odds ratio, 3.0; P = 0.04), and papilledema (odds ratio, 2.1; P = 0.02). Risk factors for a decreased prepontine CSF level included papilledema (difference in median between the group of patients who died and the group of those who survived, 0.03; P = 0.01), a lower hematocrit level in patients with less prepontine CSF, as compared with those with more prepontine CSF (Spearman's correlation coefficient, −0.16; 95% confidence interval [CI], −0.30 to −0.01; P = 0.03 in the regression slope), and witnessed convulsions on admission (difference in median, 0.51; P = 0.05 by the Wilcoxon test). The third independent MRI predictor, predominantly posterior involvement, was associated with an increased white-cell count and a decreased platelet count and with three EEG features: absence of reactivity (P = 0.004) and, as compared with patients without predominantly posterior involvement, lower average background amplitude (P = 0.04) and a slower dominant background rhythm frequency (P = 0.03).

RELATIONSHIP OF DEATH WITH BRAIN SWELLING

Of the 25 children who died, 21 (84%) had evidence of severely increased brain volume on the MRI scan at admission (odds ratio for brain swelling among patients who died vs. those who survived, 14.0; 95% CI, 4.5 to 43.4); all 21 died from respiratory arrest, consistent with the effects of increased intracranial pressure. Of the 4 patients without increased brain volume at admission, 3 died from respiratory arrest within 24 hours after admission but had not undergone a second MRI that could have detected a subsequent increase in brain volume if such an increase had occurred. The fourth patient died 17 days after admission from complications associated with HIV infection. By contrast, 39 of 143 survivors (27%) had evidence of severely increased brain volume on admission.

CHANGES IN BRAIN SWELLING OVER TIME

A total of 35 patients (5 children who died and 30 who survived) underwent a second MRI within 30 hours after the initial scan. Prepontine CSF levels decreased over time in the patients who died, whereas this measurement remained the same or increased in the patients who survived. The difference in trends was significant (P = 0.02) (Fig. 3).

DISCUSSION

Increased intracranial pressure has long been suspected to contribute to the pathogenesis of cerebral malaria in children. Uncertainty regarding its role has been exacerbated by disease heterogeneity, underpowered clinical trials,[32] misclassification, and the paucity of large studies comparing the relevant features of patients who survive with the features of those who do not. Our study design addressed the sources of this uncertainty, and the findings suggest that brain swelling and the likely increase in intracranial pressure that is associated with brain swelling are strong predictors of death in Malawian children with cerebral malaria.

Some children with cerebral malaria have clinical signs consistent with brain-stem compromise as a result of raised intracranial pressure.[12] Increased intracranial pressure, measured directly, has been observed in children with cerebral malaria,[12,23] and in one study, CT scans showed increased brain volumes in 6 of 14 children.[24] At the time of those previous studies, the importance of retinopathy status was not known, and all the children underwent scanning more than 40 hours after admission, which may have been too late to identify brain swelling. In our study, all the deaths from malaria occurred within 48 hours after admission, and the brain volumes, as assessed by means of MRI, had decreased in the 4 survivors with retinopathy-positive cerebral malaria who were still comatose 40 hours after admission. One limitation of our study is that 15 children with retinopathy-positive cerebral malaria died before undergoing an MRI, and their MRI findings may have been different from those in the patients who did undergo MRI (Table S4 in the Supplementary Appendix).

Of the imaging features specific to children with cerebral malaria,[28] severely increased brain volume was the feature most strongly associated with a fatal outcome (Table 2). The combination of three MRI features, each related to brain swelling, and one EEG finding, also associated with increased intracranial pressure and low survival rates after brain injury,[33–35] generated a model, derived exclusively from this data set, that predicted a fatal outcome (area under the ROC curve, 0.9); however, this model needs further confirmation.

The majority of patients with severely increased brain volume had decreased CSF in the prepontine space, and the most likely cause of death in this group was brain-stem herniation. A smaller subgroup of patients with brain swelling did not have a decrease in the prepontine CSF (Fig. 2). In this subgroup, an unusual pattern of posterior cerebral predominance was noted on the MRI. This pattern may result from transient occlusion of the internal cerebral vein and the vein of Galen[36] as a consequence of sequestration in postcapillary venules of the deep venous system. Among 24 patients with the posterior predominant pattern, 14 had an increased signal in the thalami on T_2-weighted MRI (Fig. 1F), a finding that is consistent with venous obstruction.[37] The high mortality in the group with predominantly posterior involvement was probably related to the hemodynamic consequences of raised intracranial pressure. The fact that two distinct groups, with MRI features and clinical risk factors that differed from each other, comprised the high-risk subgroup of children with cerebral malaria with increased brain volume suggests that different mechanisms may contribute to brain swelling.

The unifying feature in the pathogenesis of malaria is the sequestration of parasitized erythrocytes in the microvasculature of various organs. Four mechanisms could, individually or in combination, result in increased brain volume as a result of sequestration. Two involve the brain parenchyma. Cytotoxic edema could result from impaired perfusion, metabolic injury, and cell death,[28,38] whereas vasogenic edema and inflammation could be caused by endothelial-cell activation leading to disruption of the blood–brain barrier.[11,39] Two other mechanisms could increase brain volume by increasing cerebral blood volume. Intense sequestration in postcapillary venules could lead to venous obstruction and vascular congestion,[40] and the anemia, seizures, and fever that are characteristic of cerebral malaria in children could lead to increased cerebral blood flow (hyperemia) and dysfunction of autoregulatory systems.[41] Interventions targeting these mechanisms (e.g., glucocorticoids,

osmotic agents, elevation of the head of the bed, and aggressive management of fevers and seizures) would be feasible in areas where malaria is endemic.

Why was the mechanism of severely increased brain volume leading to herniation not appreciated at autopsy? Classically, the hallmarks of brain swelling and herniation on gross pathological examination are petechiae and grooving of the cerebellar tonsils as they are forced through the foramen magnum or the uncinate processes of the temporal lobes as they are forced over the tentorium. In a series of autopsies performed in Malawi, most of the patients who died from cerebral malaria and most of the comatose patients who died from nonmalarial illnesses had evidence of substantially increased brain volume,[6,21] and signs of herniation were noted in 22% of the patients,[42] but since brain swelling was nearly ubiquitous and comparisons with survivors were impossible, the relevance was not appreciated. The paucity of classic gross pathological findings may be a result of the rapidity with which death ensues in young children after brain-stem compromise when mechanical ventilatory support is not available,[43] combined with the fact that the calvaria must be removed before the base of the brain can be examined.

Brain swelling is not inevitably fatal. In our study, approximately 65% of the children with severely increased brain volume survived. Among survivors, the volume increase was transient, and the long-term outcomes were similar to those observed in survivors with normal brain volumes, suggesting that interventions that decrease brain swelling or sustain respiration temporarily, while the brain is swollen, may reduce mortality without increasing morbidity.

Supplementary Material

Refer to Web version on PubMed Central for supplementary material.

Acknowledgments

Supported by a grant (5R01AI034969) from the National Institutes of Health and by a Strategic Award for the Malawi– Liverpool–Wellcome Clinical Research Programme from the Wellcome Trust U.K. General Electric Healthcare donated the Signa 0.35-T magnetic resonance imager (MRI) used in this work, and the Michigan State University College of Osteopathic Medicine sponsored the construction of the building that houses the MRI in Malawi.

We thank the children and their parents and guardians for participation in the study; the many skilled nurses and clinicians who provided clinical care for the children on the research ward; Dr. E. James Potchen, Professor Emeritus in the Department of Radiology at Michigan State University, for wide-ranging vision and support; Ms. Careen Loos for assistance with earlier versions of the figures; Mr. Matt Latourette for technical support; Dr. Ian MacCormick for insights regarding cerebral vasculature; Dr. Michael S. Barry for feedback on an earlier version of the manuscript; and Drs. Joyce DeJong, Rudy Castellani, Kiran Thakur, and Kevin DeMarco for help with data interpretation.

REFERENCES

1. World malaria report. Geneva: World Health Organization; 2014. http://www.who.int/malaria/publications/world_malaria_report/en
2. Dondorp A, Nosten F, Stepniewska K, Day N, White N. Artesunate versus quinine for treatment of severe falciparum malaria: a randomised trial. Lancet. 2005; 366:717–725. [PubMed: 16125588]

3. Dondorp AM, Fanello CI, Hendriksen IC, et al. Artesunate versus quinine in the treatment of severe falciparum malaria in African children (AQUAMAT): an open-label, randomised trial. Lancet. 2011; 376:1647–57. [Erratum, Lancet 2011;377:126.]. [PubMed: 21062666]
4. Dondorp AM, Lee SJ, Faiz MA, et al. The relationship between age and the manifestations of and mortality associated with severe malaria. Clin Infect Dis. 2008; 47:151–157. [PubMed: 18533842]
5. Hawkes M, Elphinstone RE, Conroy AL, Kain KC. Contrasting pediatric and adult cerebral malaria: the role of the endothelial barrier. Virulence. 2013; 4:543–555. [PubMed: 23924893]
6. Taylor TE, Fu WJ, Carr RA, et al. Differentiating the pathologies of cerebral malaria by postmortem parasite counts. Nat Med. 2004; 10:143–145. [PubMed: 14745442]
7. MacPherson GG, Warrell MJ, White NJ, Looareesuwan S, Warrell DA. Human cerebral malaria: a quantitative ultra-structural analysis of parasitized erythrocyte sequestration. Am J Pathol. 1985; 119:385–401. [PubMed: 3893148]
8. White NJ, Warrell DA, Looareesuwan S, Chanthavanich P, Phillips RE, Pongpaew P. Pathophysiological and prognostic significance of cerebrospinal-fluid lactate in cerebral malaria. Lancet. 1985; 1:776–778. [PubMed: 2858665]
9. Turner GD, Ly VC, Nguyen TH, et al. Systemic endothelial activation occurs in both mild and severe malaria: correlating dermal microvascular endothelial cell phenotype and soluble cell adhesion molecules with disease severity. Am J Pathol. 1998; 152:1477–1487. [PubMed: 9626052]
10. Elhassan IM, Hviid L, Satti G, et al. Evidence of endothelial inflammation, T cell activation, and T cell reallocation in uncomplicated *Plasmodium falciparum* malaria. Am J Trop Med Hyg. 1994; 51:372–379. [PubMed: 7524374]
11. Brown H, Hien TT, Day N, et al. Evidence of blood-brain barrier dysfunction in human cerebral malaria. Neuropathol Appl Neurobiol. 1999; 25:331–340. [PubMed: 10476050]
12. Newton CR, Crawley J, Sowumni A, et al. Intracranial hypertension in Africans with cerebral malaria. Arch Dis Child. 1997; 76:219–226. [PubMed: 9135262]
13. Clark IA, Rockett RA, Cowden WB. TNF in cerebral malaria. Q J Med. 1993; 86:217–218. [PubMed: 8483997]
14. Clark IA, Cowden WB, Rockett KA. Nitric oxide in cerebral malaria. J Infect Dis. 1995; 171:1068–1069. [PubMed: 7706793]
15. Clemens R, Pramoolsinsap C, Lorenz R, Pukrittayakamee S, Bock HL, White NJ. Activation of the coagulation cascade in severe falciparum malaria through the intrinsic pathway. Br J Haematol. 1994; 87:100–105. [PubMed: 7947233]
16. Hemmer CJ, Kern P, Holst FG, et al. Activation of the host response in human *Plasmodium falciparum* malaria: relation of parasitemia to tumor necrosis factor/cachectin, thrombin-antithrombin III, and protein C levels. Am J Med. 1991; 91:37–44. [PubMed: 1858827]
17. Jimmy EO, Saliu I, Ademowo O. Fibrinopeptide-A and fibrinogen interactions in acute, *Plasmodium falciparum* malaria. Ann Trop Med Parasitol. 2003; 97:879–881. [PubMed: 14754502]
18. Mohanty D, Ghosh K, Nandwani SK, et al. Fibrinolysis, inhibitors of blood coagulation, and monocyte derived coagulant activity in acute malaria. Am J Hematol. 1997; 54:23–29. [PubMed: 8980257]
19. Moxon CA, Wassmer SC, Milner DA Jr, et al. Loss of endothelial protein C receptors links coagulation and inflammation to parasite sequestration in cerebral malaria in African children. Blood. 2013; 122:842–851. [PubMed: 23741007]
20. World Health Organization Communicable Diseases Cluster. Severe falciparum malaria. Trans R Soc Trop Med Hyg. 2000; 94(Suppl 1):S1–S90. [PubMed: 11103309]
21. Beare NA, Lewallen S, Taylor TE, Mo-lyneux ME. Redefining cerebral malaria by including malaria retinopathy. Future Microbiol. 2011; 6:349–355. [PubMed: 21449844]
22. Lewallen S, Bronzan RN, Beare NA, Harding SP, Molyneux ME, Taylor TE. Using malarial retinopathy to improve the classification of children with cerebral malaria. Trans R Soc Trop Med Hyg. 2008; 102:1089–1094. [PubMed: 18760435]
23. Newton CR, Kirkham FJ, Winstanley PA, et al. Intracranial pressure in African children with cerebral malaria. Lancet. 1991; 337:573–576. [PubMed: 1671941]

24. Newton CR, Peshu N, Kendall B, et al. Brain swelling and ischaemia in Kenyans with cerebral malaria. Arch Dis Child. 1994; 70:281–287. [PubMed: 8185359]
25. Taylor TE. Caring for children with cerebral malaria: insights gleaned from 20 years on a research ward in Malawi. Trans R Soc Trop Med Hyg. 2009; 103(Suppl 1):S6–S10. [PubMed: 19128813]
26. Barrow, GI.; Feltham, RKA., editors. Cowan and Steel's manual for the identification of medical bacteria. 3rd ed. Cambridge, United Kingdom: Cambridge University Press; 1993.
27. Potchen MJ, Kampondeni SD, Ibrahim K, et al. NeuroInterp: a method for facilitating neuroimaging research on cerebral malaria. Neurology. 2013; 81:585–588. [PubMed: 23918861]
28. Potchen MJ, Kampondeni SD, Seydel KB, et al. Acute brain MRI findings in 120 Malawian children with cerebral malaria: new insights into an ancient disease. AJNR Am J Neuroradiol. 2012; 33:1740–1746. [PubMed: 22517285]
29. Hirsch LJ, Brenner RP, Drislane FW, et al. The ACNS subcommittee on research terminology for continuous EEG monitoring: proposed standardized terminology for rhythmic and periodic EEG patterns encountered in critically ill patients. J Clin Neurophysiol. 2005; 22:128–135. [PubMed: 15805813]
30. R: a language and environment for statistical computing. Vienna: R Foundation for Statistical Computing; 2011.
31. Romano A, Bozzao A, Bonamini M, et al. Diffusion-weighted MR imaging: clinical applications in neuroradiology. Radiol Med. 2003; 106:521–548. [PubMed: 14735019]
32. Enwere G. A review of the quality of randomized clinical trials of adjunctive therapy for the treatment of cerebral malaria. Trop Med Int Health. 2005; 10:1171–1175. [PubMed: 16262742]
33. Bauer G, Trinka E, Kaplan PW. EEG patterns in hypoxic encephalopathies (post-cardiac arrest syndrome): fluctuations, transitions, and reactions. J Clin Neurophysiol. 2013; 30:477–489. [PubMed: 24084181]
34. Crepeau AZ, Rabinstein AA, Fugate JE, et al. Continuous EEG in therapeutic hypothermia after cardiac arrest: prog- nostic and clinical value. Neurology. 2013; 80:339–344. [PubMed: 23284064]
35. Fingelkurts AA, Fingelkurts AA, Bagnato S, Boccagni C, Galardi G. Life or death: prognostic value of a resting EEG with regards to survival in patients in vegetative and minimally conscious states. PLoS One. 2011; 6(10):e25967. [PubMed: 21998732]
36. Meder JF, Chiras J, Roland J, Guinet P, Bracard S, Bargy F. Venous territories of the brain. J Neuroradiol. 1994; 21:118–133. [PubMed: 8014657]
37. Teksam M, Moharir M, Deveber G, Shroff M. Frequency and topographic distribution of brain lesions in pediatric cerebral venous thrombosis. AJNR Am J Neuroradiol. 2008; 29:1961–1965. [PubMed: 18687742]
38. Beare NA, Harding SP, Taylor TE, Lewallen S, Molyneux ME. Perfusion abnormalities in children with cerebral malaria and malarial retinopathy. J Infect Dis. 2009; 199:263–271. [PubMed: 18999956]
39. Dorovini-Zis K, Schmidt K, Huynh H, et al. The neuropathology of fatal cerebral malaria in Malawian children. Am J Pathol. 2011; 178:2146–2158. [PubMed: 21514429]
40. Ponsford MJ, Medana IM, Prapansilp P, et al. Sequestration and microvascular congestion are associated with coma in human cerebral malaria. J Infect Dis. 2012; 205:663–671. [Erratum, J Infect Dis 2012;206:1483.]. [PubMed: 22207648]
41. Prohovnik I, Pavlakis SG, Piomelli S, et al. Cerebral hyperemia, stroke, and transfusion in sickle cell disease. Neurology. 1989; 39:344–348. [PubMed: 2927641]
42. Milner DA Jr, Whitten RO, Kamiza S, et al. The systemic pathology of cerebral malaria in African children. Front Cell Infect Microbiol. 2014; 4:104. [PubMed: 25191643]
43. Oemichem, M.; Auer, RN.; König, HG. Forensic neuropathology and neurology. Berlin: Springer-Verlag; 2006.

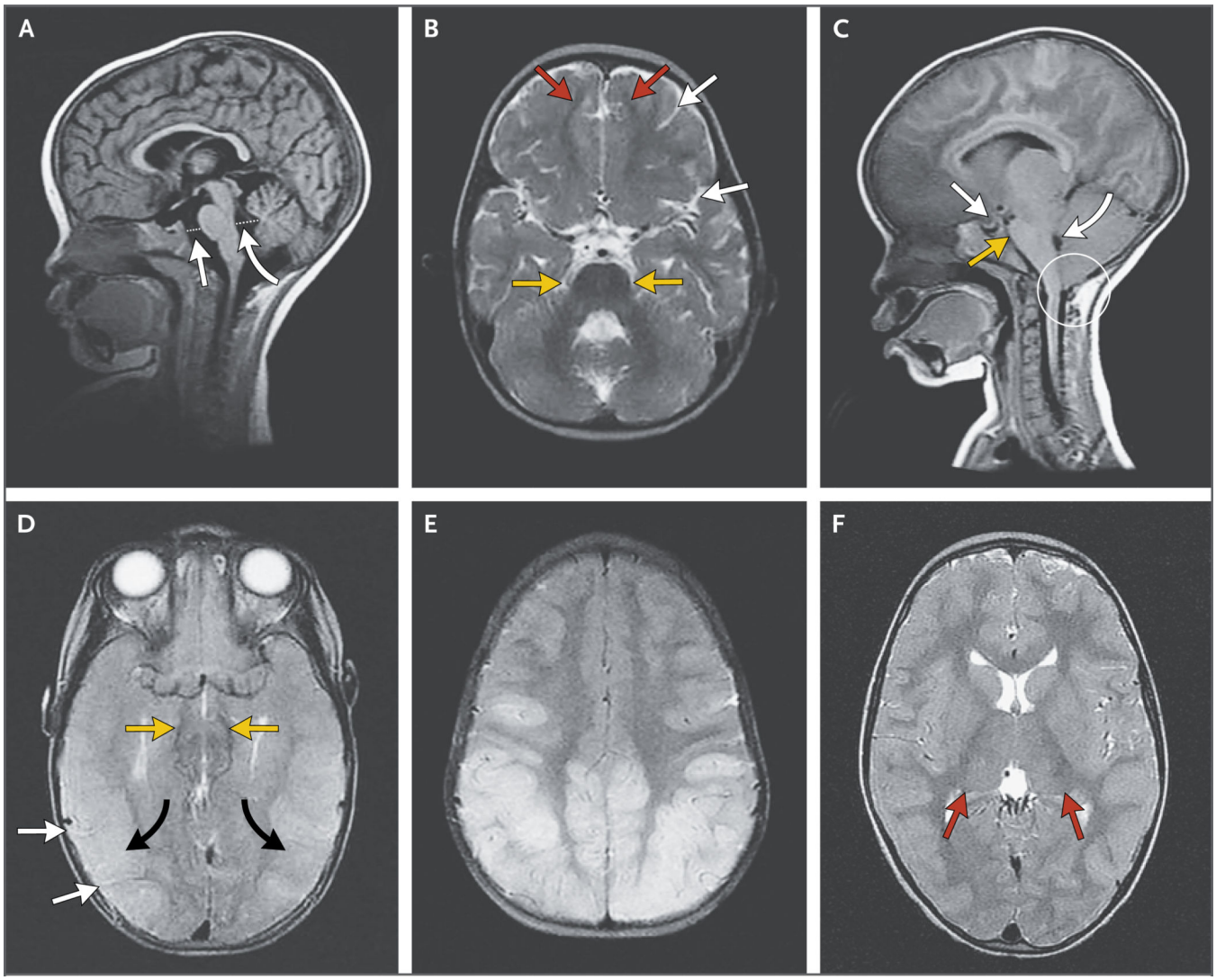

Figure 1. Brain Features on MRI in Children with Cerebral Malaria

Panel A shows normal brain volume in a 14-month-old girl at the time of a 1-month follow-up image series. This sagittal T_1-weighted MRI scan, obtained on a 0.35-T Signa Ovation Excite MRI scanner, shows how the prepontine cistern (straight arrow) and the fourth ventricle (curved arrow) are measured. Dotted lines indicate the anterior– posterior dimension of the postpontine cistern, which quantifies cerebrospinal fluid (CSF) in the fourth ventricle, and the anterior–posterior dimension of the prepontine space, which represents CSF in the subarachnoid space. The axial T_2-weighted fast spin–echo image in Panel B shows the normal appearance of the sulcal markings (white arrows), junction of gray and white matter (red arrows), and the ambient cisterns (yellow arrows). Panel C shows severely increased brain volume in a 19-month-old girl with retinopathy-positive cerebral malaria. This sagittal T_1-weighted MRI image shows downward herniation of the cerebellar tonsils (circle), effacement of the prepontine cistern (yellow arrow), and compression of the fourth ventricle (curved white arrow). There is also downward displacement of the diaphragmatic sella (straight white arrow). In Panel D, an axial T_2-weighted fast spin–echo

image of the same patient shows complete effacement of all sulcal markings (white arrows) and effacement of the ambient cisterns (yellow arrows). Marked cortical thickening and increased signal are seen diffusely throughout the visualized cortexes (black arrows). The patient survived but had a protracted recovery and was blind and deaf at discharge. The posterior predominant pattern is shown in the axial T_2-weighted fast spin–echo image in Panel E. Panel F shows an increased T_2-weighted signal in the thalami bilaterally (red arrows).

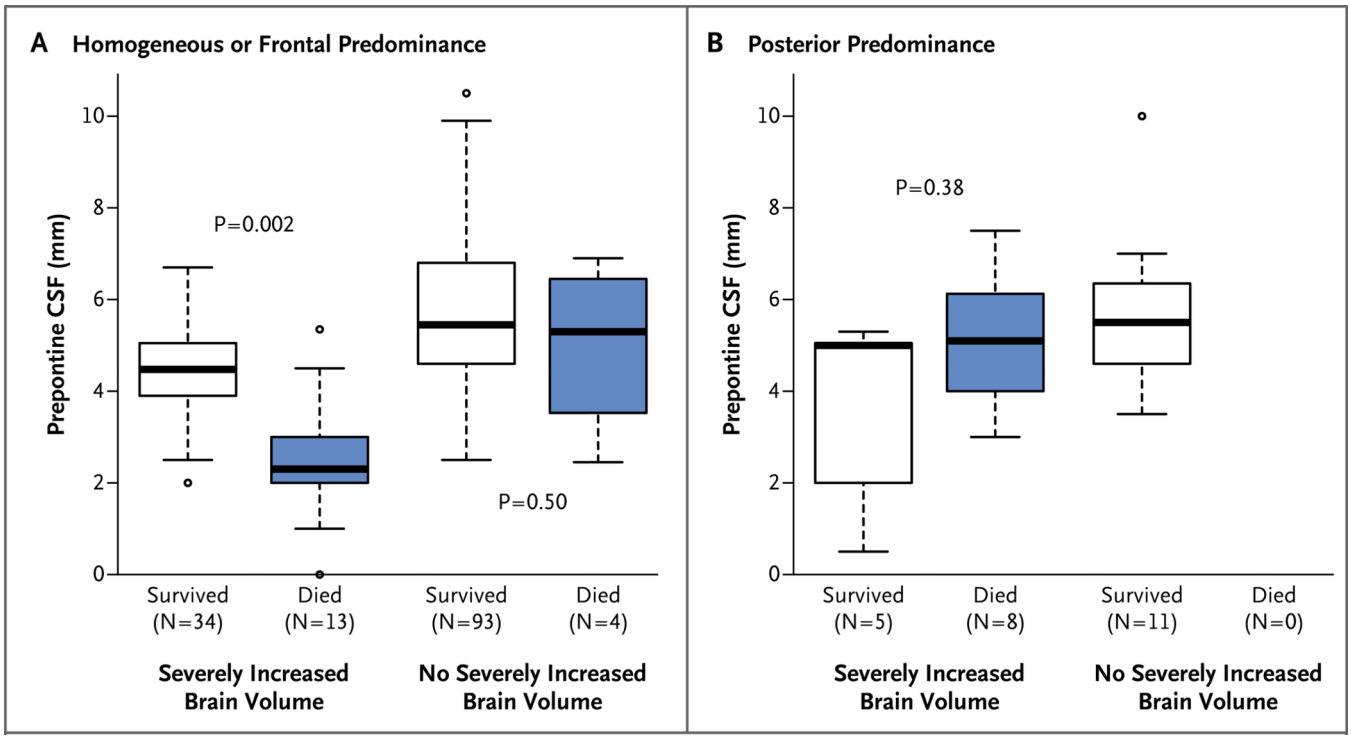

Figure 2. MRI Features Associated with a Fatal Outcome in Children with Retinopathy-Positive Cerebral Malaria

This model identified brain swelling, a decreased level of CSF in the prepontine space, and a predominantly posterior pattern of involvement as independent predictors of death. Panel A shows data for 144 patients without the posterior predominant pattern; in this group, 13 of 17 deaths occurred in patients with severely increased brain volume, and all 13 of these patients had decreased prepontine CSF. The 4 patients who died without brain swelling did not have a decreased level of prepontine CSF. Panel B shows data for the 24 patients with predominantly posterior involvement on MRI: 8 of these patients died, all of whom had increased brain volume. None of the 8 patients had decreased prepontine CSF. Solid lines indicate medians, and the boxes show interquartile ranges. Whiskers extend to 1.5 times the interquartile range, and outliers are represented individually by circles beyond the whiskers. P values comparing the prepontine CSF level between patients who survived and those who died in each subgroup were estimated by means of Wilcoxon rank-sum tests.

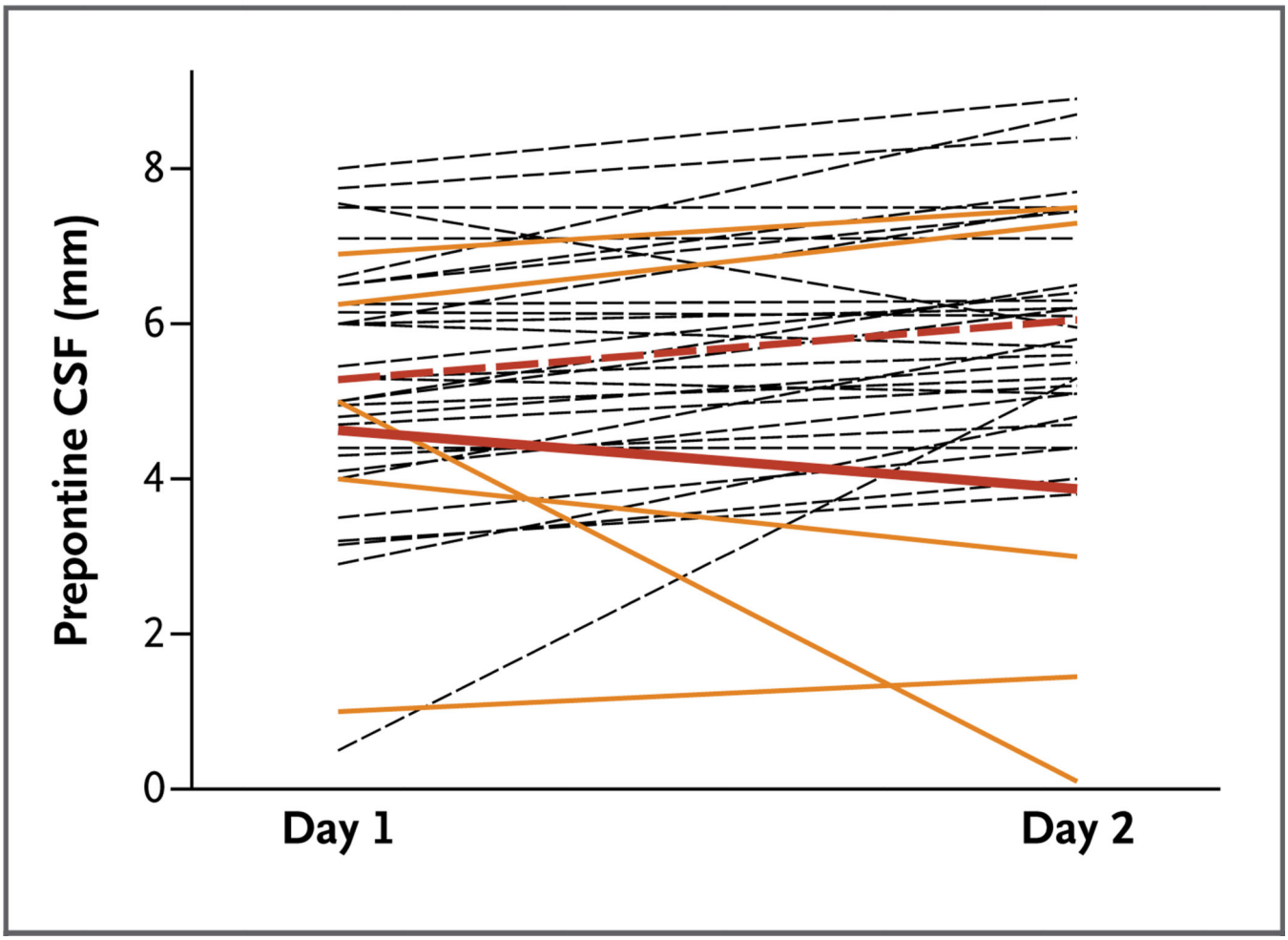

Figure 3. Distribution of Prepontine CSF Measurements on First and Second MRIs

Second MRI scans were obtained 16 to 30 hours after the first scans. Dashed black lines indicate patients who survived, and solid yellow lines patients who died. The postadmission change in the mean prepontine CSF measurement in the 30 patients with retinopathy-positive cerebral malaria who recovered and were discharged (dashed red line) was significantly different from that in the 5 patients who died (solid red line) (P = 0.02). The means and P values in the test of differences in the trajectory of the measure between the two scans were estimated with the use of a mixed model that included a random intercept to account for within-participant correlation.

Table 1

Association of Clinical and Laboratory Findings at Admission with the Subsequent Risk of Death among Patients with Retinopathy-Positive Cerebral Malaria Who Underwent MRI on Admission.*

Characteristic	Patients Who Survived (N = 143)	Patients Who Died (N = 25)	P Value†
Age — mo	52±27	50±30	0.76
Male sex — no. (%)	74 (52)	11 (44)	0.52
Mid-upper-arm circumference — cm	15.1±1.7	14.9±1.6	0.57
Weight — kg	14±5	13±4	0.39
Height — cm	98±16	95±14	0.39
Variable before admission			
Duration of fever — hr	64.2±32.3	55.3±31.6	0.21
Duration of coma — hr	15.6±20.8	14.5±15.4	0.76
History of seizure — no. (%)	123 (86)	20 (80)	0.32
Temperature — °C	38.8±1.2	38.8±1.3	0.94
Pulse rate — beats/min	152±24	156±26	0.47
Respiratory rate — breaths/min	44±11	47±12	0.20
Liver size — cm below costal margin	1.4±1.6	1.7±1.6	0.32
Jaundice — no. (%)	12 (8)	3 (12)	0.47
Spleen size — cm below costal margin	0.9±1.4	0.7±1.2	0.73
Deep breathing — no. (%) Blantyre coma score — no. (%)‡	29 (20)	5 (20)	1.00
			0.09
0	13 (9)	2 (8)	
1	71 (50)	15 (60)	
2	59 (41)	8 (32)	
Seizure at time of admission — no. (%)	28 (20)	4 (16)	0.79§
CSF opening pressure — mm of water¶			0.33
Median	140	170	
Interquartile range	100–180	119–230	
Papilledema — no./total no. (%)	46/139 (33)	10/25 (40)	0.50
Hematocrit — %	20.8±5.6	20.9±4.6	0.89
Platelets — $\times 10^{-9}$/liter			0.17
Median	54	46	
Interquartile range	34–87	25–71	
Parasitemia — parasites/mm^3			0.23
Median	55,778	71,280	
Interquartile range	12,660–220,000	31,680–528,000	
White cells — $\times 10^{-9}$/liter			0.05
Median	8.4	11.7	

Characteristic	Patients Who Survived (N = 143)	Patients Who Died (N = 25)	P Value[†]
Interquartile range	6.6–12.7	6.7–19.4	
Sodium — mmol/liter[//]	136.3±7.4	136.0±4.7	0.89
Lactate — mmol/liter	6.8±4.2	9.8±4.2	0.001
Blood glucose — mmol/liter[**]	6.3±2.9	6.8±3.5	0.52
CSF white-cell count			
≥5 — no./total no. (%)	13/107 (12)	3/15 (20)	0.42[§]
Count in patients with value ≥5			0.70
Median	7	9	
Interquartile range	5–10	6–12	
HIV positive — no./total no. (%)	17/130 (13)	2/21 (10)	0.75[§]

[*] Plus–minus values are means ±SD. No cerebrospinal fluid (CSF) or blood cultures resulted in growth of a pathogen. HIV denotes human immunodeficiency virus.

[†] P values were estimated with the use of Student's t-tests for means, Wilcoxon rank-sum tests for medians, and Pearson's chi-square tests for proportions, except when noted otherwise.

[‡] The scale for the Blantyre coma score ranges from 0 to 5, with lower scores indicating decreased levels of consciousness.

[§] The P value was estimated with the use of Fisher's exact test.

[¶] A total of 107 children who survived and 15 children who died underwent CSF analysis.

[//] Data were available for 136 patients who survived and for 12 who died.

[**] Data were available for patients who did not receive dextrose before admission (115 of the patients who survived and 19 of those who died). To convert the values for blood glucose to milligrams per deciliter, divide by 0.05551.

Table 2

Associations of MRI and EEG Abnormalities with Death in Patients with Retinopathy-Positive Cerebral Malaria.*

Finding on MRI or EEG	Patients Who Survived (N = 143)	Patients Who Died (N = 25)	Single Covariate Regression Analysis		Multiple Regression Analysis†	
			Odds Ratio (95% CI)	P Value‡	Odds Ratio (95% CI)	P Value‡
Abnormality on MRI						
Brain-volume indicator						
Severely increased brain volume (no.)§	39	21	14.0 (4.5–43.4)	<0.001	7.5 (2.1–26.9)	<0.001
Postpontine CSF (mm)			0.7 (0.6–0.9)	<0.001	—	
Median	10.0	8.5				
Interquartile range	8.7–11.3	6.8–9.9				
Prepontine CSF (mm)			0.5 (0.4–0.7)	<0.001	0.5 (0.3–0.8)	<0.001
Median	5.1	3.6				
Interquartile range	4.4–6.5	2.3–5.2				
Increased signal on T_2-weighted imaging (no)¶						
Subcortical white matter	106	16	0.6 (0.2–1.5)	0.29	—	—
Periventricular white matter	47	11	1.6 (0.7–3.8)	0.28	—	—
Thalamus	64	17	2.6 (1.1–6.5)	0.03	—	—
Cortical gray matter	119	24	4.8 (0.6–37.5)	0.13‖	—	—
Posterior fossa	92	19	1.8 (0.7–4.7)	0.26	—	—
Corpus callosum	66	9	0.7 (0.3–1.6)	0.35	—	—
Pons	72	15	1.5 (0.6–3.5)	0.37	—	—
Brain stem	92	20	2.2 (0.8–6.3)	0.13	—	—
Basal ganglia	116	23	2.7 (0.6–12.0)	0.26‖	—	—
Increased signal on diffusion-weighted imaging (no.)**						
Supratentorial white matter	63	6	0.4 (0.2–1.1)	0.07	—	—
Supratentorial gray matter	10	10	9.4 (3.3–26.4)	<0.001	—	—

Finding on MRI or EEG	Patients Who Survived (N = 143)	Patients Who Died (N = 25)	Single Covariate Regression Analysis		Multiple Regression Analysis†	
			Odds Ratio (95% CI)	P Value‡	Odds Ratio (95% CI)	P Value‡
Posterior fossa	7	1	0.8 (0.1–7.1)	1.0//	—	—
Corpus callosum	52	5	0.4 (0.2–1.3)	0.12	—	—
Basal ganglia	41	7	1.0 (0.4–2.6)	0.99	—	—
Anatomical variables on T_2-weighted or diffusion-weighted imaging (no.)						
Posterior fossa						
Involved	11	2	1.0 (0.2–5.0)	1.0	—	
Spared	44	9	1.3 (0.5–3.1)	0.60	—	
Posterior predominance	16	8	3.6 (1.6–9.8)	0.01//	3.4 (0.9–12.7)	0.02
Patchy lesions††	9	7	3.4 (1.4–8.4)	0.006//	—	
EEG finding						
Clinical or subclinical seizure activity (no.)	88	18	1.6 (0.6–4.6)	0.32	—	
Normal sleep architecture (no.)	53	3	0.2 (0.0–0.6)	0.006	—	
Reactivity (no.)	52	3	0.2 (0.0–0.6)	0.003	—	
Dominant rhythm frequency (Hz)						
Median	2.5	1.5	0.4 (0.2–0.7)	<0.001	0.3 (0.2–0.6)	<0.001
Interquartile range	1.5–3.3	1.5–2.0				
Average background amplitude (mV)						
Median	100	80	1.0 (1.0–1.0)	0.08	—	
Interquartile range	80–150	50–120				

*Comparisons were performed with the use of single covariate and multiple logistic-regression analyses. The model presented here had a Hosmer–Lemeshow chi-square of 0.68 and a C-statistic of 0.90. CI denotes confidence interval, and EEG electroencephalogram.

†No clinical or laboratory covariate was a significant predictor of death or increased the C-statistic in models that included relevant MRI and EEG features. The multivariate analysis included 124 patients who survived and 25 who died; 19 patients who did not undergo EEG were excluded.

‡P values in the single covariate analysis were estimated with the use of Pearson's chi-square test (or Fisher's exact test, where noted) for categorical variables and with the use of the Wilcoxon rank-sum test for continuous variables. P values in the multiple regression analysis were estimated with the use of likelihood-ratio tests.

[§] Severely increased brain volume was defined as a volume score of 7 or 8, as compared with a score of 1 to 6. Overall brain volume was scored on the basis of the appearance of the cerebral hemispheres on a scale from 1 to 8, with a score of 1 indicating marked atrophy, 2 mild atrophy, 3 normal volume, 4 slightly increased volume, 5 mildly increased volume, 6 obvious but moderate levels of increased brain volume, 7 substantially increased volume with diffuse sulcal and cisternal effacement but no evidence of herniation, and 8 sulcal and cisternal effacement with evidence of herniation. The risk of death associated with the patients' scores was as follows: score of 2, 0%; score of 3, 0%; score of 4, 8%; score of 5, 4%; score of 6, 4%; score of 7, 31%, and score of 8, 55% ($P<0.001$ for all comparisons for the association with death). No patient had a score of 1 in this study.

[¶] An increased signal on T_2-weighted imaging indicates increased water within the affected brain tissue.

[//] The P value was estimated with the use of Fisher's exact test.

[**] An increased signal on diffusion-weighted imaging without an increased signal on T_2-weighted imaging represents restricted diffusion of water molecules.[31]

[††] Patchy lesions were defined as focal areas of pronounced lobar involvement, as assessed on T_2-weighted imaging, and may represent discrete areas of cerebral injury or involvement, possibly related to localized cerebritis on a backdrop of diffuse venous occlusion. Confluent lesions may represent diffuse venous occlusion only.